bioRxiv preprint doi: https://doi.org/10.1101/178491; this version posted August 19, 2017. The copyright holder for this preprint (which was not certified by peer review) is the author/funder. All rights reserved. No reuse allowed without permission.

1 # The effect of sonic hedgehog on motor neuron positioning in the
2 # spinal cord during chicken embryo development

3 Ciqing Yang[1,2], Xiaoying Li[1], Qiuling Li[1], Qiong Li[2], Han Li[3], Bichao Zhang[1,2], Juntang Lin[1,2,4,5*]

4 1 Stem Cells & Biotherapy Engineering Research Center of Henan, College of Life Science and
5 Technology, Xinxiang Medical University, 453003 Xinxiang, China
6 2 Henan Key Laboratory of Medical Tissue Regeneration, 453003 Xinxiang, China
7 3 Advanced Medical and Dental Institute, University Sains Malaysia, Bertam, Penang 13200,
8 Malaysia
9 4 College of Biomedical Engineering, Xinxiang Medical University, 453003 Xinxiang, China
10 5 Institute of Anatomy I, Jena University Hospital, 07743-Jena, Germany

11

12 Running title: The effect of sonic hedgehog on motor neuron positioning

13 *Corresponding author: Dr. Juntang Lin
14 College of Biomedical Engineering, Xinxiang Medical University, 453003 Xinxiang,
15 China;
16 Email: developmentlab@126.com

17

bioRxiv preprint doi: https://doi.org/10.1101/178491; this version posted August 19, 2017. The copyright holder for this preprint (which was not certified by peer review) is the author/funder. All rights reserved. No reuse allowed without permission.

18 **ABSTRACT**

19 Sonic hedgehog (Shh) is a vertebrate homologue of the secreted *Drosophila* protein
20 hedgehog, and is expressed by the notochord and the floor plate in the developing
21 spinal cord. Shh provides signals relevant for positional information, cell proliferation,
22 and possibly cell survival depending on the time and location of the expression.
23 Although the role of Shh in providing positional information in the neural tube has
24 been experimentally proven, the exact underlying mechanism still remains unclear. In
25 this study, we report that overexpression of Shh affects motor neuron positioning in
26 the spinal cord during chicken embryo development by inducing abnormalities in the
27 structure of the motor column and motor neuron integration. In addition, Shh
28 overexpression inhibits the expression of dorsal transcription factors and commissural
29 axon projections. Our results indicate that correct location of Shh expression is the
30 key to the formation of the motor column. In conclusion, the overexpression of Shh in
31 the spinal cord not only affects the positioning of motor neurons, but also induces
32 abnormalities in the structure of the motor column.

33

34 **Key words:** Sonic hedgehog; in ovo electroporation; motor neurons; spinal cord;
35 chicken embryo

bioRxiv preprint doi: https://doi.org/10.1101/178491; this version posted August 19, 2017. The copyright holder for this preprint (which was not certified by peer review) is the author/funder. All rights reserved. No reuse allowed without permission.

36 **INTRODUCTION**

37 During central nervous system development, many factors can be controlled to ensure
38 normal development. The early embryonic vertebrate neural tube consists of
39 proliferating progenitors and terminally differentiating neurons with a defined
40 distribution pattern (Cayuso et al., 2006). The notochord and floor plate at the ventral
41 midline of the neural tube determine, in part, the organization of the developing spinal
42 cord (Pringle et al., 1996). These structures also emit signals that can induce the
43 development of distant motor neurons (Yamada et al., 1991, 1993; Tanabe et al.,
44 1995). In the ventral spinal cord, motor neurons (MN) are grouped in motor columns
45 according to their identity and their target muscle (Luxey et al., 2015). Different
46 motor neurons express different sets of transcription factors. For instance, HB9 is
47 expressed in all somatic MN, whereas Foxp1, Lim1, and Islet1 are all expressed in
48 lateral motor column MN at high levels (Vermot et al., 2005; Bonanomi and Pfaff,
49 2010; Santiago et al., 2014; Luxey et al., 2015). All these transcription factors have
50 been shown to contribute to the establishment of MN organization in the spinal cord.
51 Indeed, gain and loss of function of HB9, Islet1, Islet2, Lim1, and Foxp1 lead to
52 important defects of MN positioning within the spinal cord during embryo
53 development (Kania et al., 2000; Odden et al., 2002; Bréjot et al., 2006; Hutchinson
54 and Eisen, 2006; Rousso et al., 2008; Otaegi et al., 2011). Although the role of these
55 transcription factors in MN positioning in the spinal cord is well established, little is
56 known regarding their potential effector genes (Luxey et al., 2015).
57 Sonic hedgehog (Shh) is a vertebrate homologue of the secreted protein encoded by

bioRxiv preprint doi: https://doi.org/10.1101/178491; this version posted August 19, 2017. The copyright holder for this preprint (which was not certified by peer review) is the author/funder. All rights reserved. No reuse allowed without permission.

58 the *Drosophila* gene hedgehog (Lee et al., 1992; Nusslein-Volhard et al., 1980), and is
59 expressed by the notochord and floor plate at the time when these structures exert
60 their inductive activities (Riddle et al., 1993; Echelard et al., 1993). In the central
61 nervous system, Shh plays an important role in ventral specification along the entire
62 neural axis. In ventral regions, this protein acts as a long-range graded signal that
63 controls the pattern of neurogenesis (Jessell, 2000; Briscoe and Ericson, 2001).
64 Misexpression of Shh in vertebrate embryos can induce the differentiation of floor
65 plate cells at ectopic locations in the neural tube (Echelard et al., 1993; Krauss et al.,
66 1993; Roelink et al., 1994). Shh provides signals relevant to positional information,
67 cell proliferation, and possibly cell survival depending on the timing and location of
68 the expression (Riddle et al., 1993; Peterson et al., 2012; Yang et al., 2015). Although
69 the role of Shh in providing positional information in the neural tube has been
70 experimentally established, the mechanism underlying this phenomenon remains
71 unclear.
72 In this study, we focus on the role of Shh in motor neuron positioning in the spinal
73 cord during chicken embryo development by inducing its misexpression in the
74 embryonic spinal cord. We examined the gene expression in Shh-transfected spinal
75 cord and followed spinal cord development. Shh expression can directly or indirectly
76 affect the development of multiple structures. Moreover, the localization of
77 dorsal-ventral cell types was determined to analyze the effects of Shh in cell type
78 specification. The results of these studies indicated that Shh affects the expression of
79 dorsal transcription factors Pax3 and Pax7 and the positioning of ventral motor

bioRxiv preprint doi: https://doi.org/10.1101/178491; this version posted August 19, 2017. The copyright holder for this preprint (which was not certified by peer review) is the author/funder. All rights reserved. No reuse allowed without permission.

80 neurons in the spinal cord.

81

82 **RESULTS**

83 **Shh overexpression in the developing chicken spinal cord**

84 In ovo electroporation, a technique by which the plasmid can be unilaterally
85 electroporated, was performed to examine the role of Shh in the developing spinal
86 cord. Two experimental groups were designed as follows: 1) electroporation of
87 pCAGGS-GFP (0.25 μg/μL) – control group, 2) co-electroporation of pCAGGS-Shh
88 (4 μg/μL) + pCAGGS-GFP (0.25 μg/μL) - experimental group. Electroporation was
89 performed on the chicken embryonic spinal cord at stage 17 (E2.5). After 36, 60, and
90 84 h following electroporation, GFP-positive embryos were collected at stage 24-26
91 (E4-E6), and the overexpression of Shh was clearly observed using in situ
92 hybridization (Fig. 1A-C, arrows [→] indicate the areas of Shh overexpression). To
93 control for individual differences, data from the same spinal cord, where the
94 transfected and non-transfected sides served as experimental and control tissue,
95 respectively, were matched. Shh was expressed by the notochord and floor plate in the
96 developing chicken spinal cord (Fig. 1D-F). As the notochord is also known to induce
97 differentiation of other ventral cell types within the neural tube, including motor
98 neurons, it can be hypothesized that Shh produced by the notochord may be required
99 for motor neuron differentiation.

100

101 **The effect of Shh** over**expression on microtubule-associated protein-2 (Map2)**

bioRxiv preprint doi: https://doi.org/10.1101/178491; this version posted August 19, 2017. The copyright holder for this preprint (which was not certified by peer review) is the author/funder. All rights reserved. No reuse allowed without permission.

102 **expression in motor column in the developing chicken spinal cord**

103 Interestingly, MAP-2 labeling of motor columns following Shh overexpression in the
104 spinal cord revealed structural abnormalities (Fig. 2A-L, arrow shown). In the control
105 group, the structure of MAP-2 labeled motor column was normal (Fig. 2M-X).
106 MAP-2 belongs to the microtubule-associated protein family. The proteins of this
107 family are thought to participate in microtubule assembly, which is an essential step in
108 neuritogenesis. MAP-2 isoforms are found predominately in neurons (Tucker, 1990).
109 The principal functions of MAP-2 are to reduce the critical concentration of tubulin
110 required to polymerize microtubules and to maintain neuronal morphology by
111 regulating microtubule spacing (Caceres et al., 1992; Kalcheva et al., 1995). Even
112 though MAP-2 is not a specific maker for motor neurons, motor neurons express
113 MAP-2. Whether Shh overexpression affects the formation of the motor column by
114 inhibiting the expression of MAP-2 in motor neurons is unclear. DAPI staining on the
115 section slices showed a loss of cell nuclei on the transfected side of the motor column
116 compared to non-transfected side (Fig. 2A-D, E-H). In the control group, the number
117 of nuclei on the transfected side of the motor column was similar to that on the
118 non-transfected side (Fig. 2M, Q). No GFP or MAP-2 positive neurons were
119 observed in the motor column in the experimental group (Fig. 2 K-L). In the control
120 group, GFP and MAP-2 positive neurons were observed in the motor column (Fig. 2
121 U-X). Therefore, it could be speculated that Shh may not inhibit the expression of
122 MAP-2, but instead, modify the migration of motor neurons to the motor column. To
123 verify this hypothesis, we used MNR2 to label motor neurons.

bioRxiv preprint doi: https://doi.org/10.1101/178491; this version posted August 19, 2017. The copyright holder for this preprint (which was not certified by peer review) is the author/funder. All rights reserved. No reuse allowed without permission.

124

125 **The effect of Shh overexpression on motor neuron (MNR2) positioning within**
126 **the motor column in the chicken spinal cord**

127 MNR2 is expressed selectively by motor neurons (MNs) in the developing vertebrate
128 central nervous system. In order to investigate whether Shh affects the migration of
129 motor neurons, or simply inhibits the expression of MAP-2 in motor neurons, we used
130 MNR2 to specifically identify motor neurons. In the Shh overexpression group,
131 MNR2 positive cells showed decreased accumulation in the motor column on the
132 transfected side of the spinal cord as compared to the non-transfected side (Fig. 3A-H).
133 However, in the control group, the distribution of MNR2 positive cells in the motor
134 column on the transfected side was similar to that on the non-transfected side (Fig.
135 3I-P). Moreover, we observed morphological changes in the spinal cord with Shh
136 overexpression (Fig. 3A-D). The spinal cord on the transfected side was curved
137 outward, which was interpreted as the result of Shh overexpression rather than a
138 physiological phenomenon (Fig. 3E-H). On the contrary, the morphology of the GFP
139 -transfected side in the spinal cord was normal (Fig. 3I-L). In these areas, no outward
140 curving was observed (Fig. 3M-P). Outward bending of the spinal cord in the areas of
141 Shh overexpression has several potential explanations. It may be explained by the fact
142 that Shh promotes proliferation of neuroepithelial cells, which leads to bending of the
143 spinal cord outwards. In addition, these morphological changes may also be due to the
144 effect of Shh on neuronal migration, especially that of motor neurons. The distribution
145 of MNR2-labeled cells supports the effect of Shh on motor neuron migration. In order

bioRxiv preprint doi: https://doi.org/10.1101/178491; this version posted August 19, 2017. The copyright holder for this preprint (which was not certified by peer review) is the author/funder. All rights reserved. No reuse allowed without permission.

146 to investigate whether Shh can promote the proliferation of neuroepithelial cells,
147 BrdU was used to label the proliferating cells.
148
149 **The effect of Shh expression on neuroepithelial cell proliferation in the spinal**
150 **cord during chicken embryo development**
151 BrdU is a synthetic analog of thymidine commonly used for the detection of
152 proliferating cells in living tissues (Lehner et al., 2011). BrdU was added 24 h before
153 the spinal cord tissue was collected. Immunohistochemistry with anti-BrdU
154 monoclonal antibody was used to reveal BrdU-positive cells. These cells were
155 counted in the neural epithelium. The ratios of BrdU-positive cell number on the
156 experimental (transfected) side over control (non-transfected) side were analyzed (Fig.
157 4a). Such a comparison between the experimental group versus control group (as
158 shown in the Fig. 4a) indicated a significant increase in BrdU-positive cell numbers in
159 the developing chick spinal cord, from stage 17 to 24, in Shh transfected tissue (Fig.
160 4A-D). The ratio of transfected to non-transfected side was 1.57±0.22 (n=3). In the
161 control group, no difference in the number of BrdU-positive cells was observed
162 between the GFP-transfected side and the non-transfected side of the spinal cord,
163 from stage 17 to 24 (Fig. 4E-H). The ratio of transfected to non-transfected side was
164 1.12±0.14 (n=3). The ratios of transfected to non-transfected side were significantly
165 different between the Shh overexpression group and control group ($p<0.01$, Fig. 4b).
166 A comparison between the side of the spinal cord transfected with Shh and the control
167 non-transfected side (as shown in the Fig. 4c) indicated a significant decrease in

bioRxiv preprint doi: https://doi.org/10.1101/178491; this version posted August 19, 2017. The copyright holder for this preprint (which was not certified by peer review) is the author/funder. All rights reserved. No reuse allowed without permission.

168 BrdU-positive cells in the developing chick spinal cord, from stage 17 to 29 (Fig.
169 4I-L). The ratio of transfected side to non-transfected side was 0.70±0.32 (n=3). In the
170 control group, no difference in the number of BrdU-positive cells between the
171 transfected and non-transfected side in the spinal cord was observed from stage 17 to
172 29 (Fig. 4M-P). The ratio of transfected side to non-transfected side was 0.98±0.19
173 (n=3). The ratios of transfected side to non-transfected side in Shh overexpression
174 group versus control group were significantly different ($p<0.01$, Fig. 4d). The
175 decrease in the number of BrdU-labeled cells on the side with Shh overexpression
176 compared to the contralateral side was particularly visible in the ventral areas of the
177 spinal cord (Fig. 4Q-T). The ratio of transfected side to non-transfected side was
178 0.53±0.27 (n=3). In the control group, no differences were observed (Fig. 4U-X). The
179 ratio of transfected side to non-transfected side was 1.17±0.11 (n=3). As shown in Fig.
180 4e, the ratio of the number of BrdU-positive cells on the transfected side to that on the
181 non-transfected side was significantly different in the Shh overexpression group
182 compared to control group ($p<0.01$, Fig. 4f). Interestingly, in stage 24 (E4), Shh
183 promoted neuroepithelial cell proliferation (Fig. 4b), while in stage 26 (E6) it had an
184 inhibitory effect (Fig. 4d, f). Therefore, we speculated that Shh not only affects the
185 proliferation of neural precursor cells but also their differentiation. It is possible that,
186 in response to Shh misexpression in early stages of embryonic development, neural
187 precursor cells were induced to differentiate into nerve cells therefore losing their
188 ability to proliferate, which is why the number of proliferating cells was significantly
189 decreased compared to control group.

bioRxiv preprint doi: https://doi.org/10.1101/178491; this version posted August 19, 2017. The copyright holder for this preprint (which was not certified by peer review) is the author/funder. All rights reserved. No reuse allowed without permission.

190

191 **The effect of Shh overexpression on Pax3 and Pax7 expression in the spinal cord**

192 **during chicken embryo development**

193 Shh affects not only the differentiation and proliferation of ventral cells, but also the
194 expression of dorsal genes during chicken embryonic development. The expression of
195 the nuclear proteins Pax3 and Pax7 was therefore investigated. The results showed
196 that Pax3 expression was inhibited at the side of Shh overexpression position
197 compared to the control, non-transfected, side (Fig. 5A-F, arrow), which suggests that
198 early expression of Shh inhibits Pax3 expression. However, no differences in the
199 expression between the two sides of the spinal cord were observed in the control
200 group (Fig. 5G-L). Further, the mean optical density ratios of the experimental
201 (transfection) side to the control (no transfection) side were analyzed (Fig. 5a). Cell
202 numbers in the control group were significantly ($p<0.01$) higher than those in the Shh
203 overexpression group (Fig. 5 b). Pax7 expression was also inhibited at the side with
204 Shh overexpression position compared to the control non-transfected side (Fig. 5M-R,
205 arrow). No differences in Pax7 expression were observed between the transfected
206 versus non-transfected side in the control group (Fig. 5S-X). The numbers of
207 Pax7-positive cells in the control group were significantly ($p<0.01$) higher than in the
208 Shh overexpression group (Fig. 5c). Additionally, the percentage of commissural
209 axons projecting to the contralateral side in the Shh overexpression group was
210 significantly lower in comparison to the control (Fig. 5d, $p<0.01$). Therefore, our
211 results suggest that Shh overexpression may inhibit the commissural axons projecting

bioRxiv preprint doi: https://doi.org/10.1101/178491; this version posted August 19, 2017. The copyright holder for this preprint (which was not certified by peer review) is the author/funder. All rights reserved. No reuse allowed without permission.

212 to the contralateral side in the spinal cord during chicken embryo development.

213 To assess the morphological changes that are induced by shh overexpression along the
214 transfected spinal cords, the rostro-caudal series of sections were obtained. These
215 series sections result confirmed that the shh overexpression perturbed axon
216 projections (Fig 6). The shh overexpression lead to commissural axons projecting to
217 the contralateral side weak mlc and almost no ilc (Fig. 6A-G), as H shows. In the
218 control there have normal commissural axons projecting to the contralateral side and
219 axons arrived to mlc and ilc (Fig. 6I-O), as Fig 6P shows.

220 **DISCUSSION**

221 Shh is one of three proteins in the mammalian hedgehog signaling family, the others
222 being desert hedgehog and Indian hedgehog. Shh is the most studied hedgehog
223 signaling pathway. It plays a critical role in the patterning of vertebrate embryonic
224 nervous system, including the brain and the spinal cord, during development (Chiang
225 et al., 1996). Shh is a secreted protein that mediates signaling activities in the
226 notochord and the floor plate (Patten and Placzek, 2000). One of early functions of the
227 notochord is to induce differentiation of ventral cell types, such as floor plate cells
228 and motor neurons in the overlying neural ectoderm (Chiang et al., 1996). Shh is
229 considered to play an important role during spinal cord development (Martí et al.,
230 1995), given its predominant expression in the notochord and floor plate during
231 embryo development. In this study, we demonstrate that the overexpression of Shh
232 affects motor neuron positioning in the spinal cord during chicken embryo
233 development.

bioRxiv preprint doi: https://doi.org/10.1101/178491; this version posted August 19, 2017. The copyright holder for this preprint (which was not certified by peer review) is the author/funder. All rights reserved. No reuse allowed without permission.

234 Our results show that Shh overexpression affects the expression pattern of MAP-2.
235 The abnormal pattern of MAP-2 expression was not due to the inhibition by Shh, but
236 to the effect of Shh on the migration of motor neurons, preventing them from reaching
237 their positions within the motor column accurately. In order to confirm these results,
238 MNR2 labeling was performed to precisely identify motor neurons. The results
239 showed that, in the Shh overexpression group, the transfected side showed a deficit in
240 the accumulation of MNR2 positive cells in the motor column compared to
241 non-transfected side. These results were consistent with the expected ones, indicating
242 that the Shh overexpression, rather than inhibiting the expression of MAP-2, affected
243 the migration of motor neurons, which led to the absence of MAP-2 expression in the
244 motor column region. Besides Shh, factors such as HB9, Islet1, Islet2, Lim1, and
245 Foxp1, if misexpressed, could also induce defective motor neuron positioning within
246 the spinal cord during embryo development (Bréjot et al., 2006; Odden et al., 2002;
247 Hutchinson and Eisen, 2006; Kania et al., 2000; Otaegi et al., 2011; Rousso et al.,
248 2008). The mechanisms by which different molecules affect the migration of motor
249 neurons are different. Shh acts in a graded fashion to pattern the dorsal-ventral axis of
250 the vertebrate spinal cord. This is a dynamic process in which increasing
251 concentrations and the duration of exposure to Shh generate neurons with
252 successively more ventral identities (Ribes and Briscoe, 2009). Thus, Shh ligand
253 secreted by the notochord induces distinct ventral cell identities in the adjacent spinal
254 cord by a concentration-dependent mechanism (Chamberlain et al., 2009). Normally,
255 the concentration of Shh increases gradually from dorsal to ventral regions. The

bioRxiv preprint doi: https://doi.org/10.1101/178491; this version posted August 19, 2017. The copyright holder for this preprint (which was not certified by peer review) is the author/funder. All rights reserved. No reuse allowed without permission.

256 highest concentrations of the Shh ligand are found in the most ventral regions of the
257 neural tube and notochord, while lower concentrations are found in the more dorsal
258 regions of the neural tube (Ribes et al., 2009). In our experiment, the overexpression
259 of Shh in the spinal cord induced structural abnormalities in the nerve column. One
260 possibility is that motor neurons failed to migrate to the right position, possibly due to
261 high concentrations of Shh while another is that the structural abnormalities are a
262 result of the inhibition of neuroepithelial cell differentiation into motor neurons.
263 Therefore, in this study, the proliferation of neuroepithelial cells was investigated
264 using labeling with BrdU. BrdU is incorporated into newly synthesized DNA in the
265 replicating cells during the S phase of the cell cycle, as a substitute for thymidine.
266 Antibodies specific for BrdU can be used to detect this compound incorporated into
267 the DNA, thus indicating the cells with actively replicating DNA during BrdU
268 administration (proliferating cells). The results of our study show that cell
269 proliferation in the early stage (stage 18-24, E3-E4) was higher than in the late stage
270 (stage 27-29, E5-E6). Does this mean that the overexpression of Shh promotes the
271 proliferation of neuroepithelial cells in the early stage (stage 18-24, E3-E4), but
272 inhibits proliferation in the late stage (stage 27-29, E5-E6)? Studies have shown that
273 Shh acts in a concentration-dependent manner (Placzek et al., 1990) so that lower
274 concentrations of Shh promote cellular proliferation and induction of various ventral
275 neural cell types (Ericson et al., 1996), while high concentrations of Shh inhibit
276 cellular proliferation (Wilson and Maden, 2005). We believe that promoting cell
277 proliferation is only one of the effects of Shh, the other one being the promotion of

bioRxiv preprint doi: https://doi.org/10.1101/178491; this version posted August 19, 2017. The copyright holder for this preprint (which was not certified by peer review) is the author/funder. All rights reserved. No reuse allowed without permission.

278 neural precursor cell differentiation. In the early stage (stage 18-24), Shh promotes the
279 neural precursor cell differentiation into neurons, and these neurons then lose the
280 ability to proliferate. Shh affected the formation of motor neurons by inducing a
281 defect in their migration to the motor column and, consequently, altering their
282 distribution in the border of the gray matter and leading to the formation a band. The
283 ultimate result was the abnormal structure of the motor column. The effect of Shh on
284 neural precursor cell differentiation requires further research.

285 It is thought that Shh gradient determines multiple different cell fates by a
286 concentration and time-dependent mechanism that induces the expression of several
287 transcription factors in ventral progenitor cells (Chamberlain et al., 2008). In this
288 study, we examined the expression of dorsal transcription factors Pax3 and Pax7. Our
289 results showed that the expression of Pax3 and Pax7 was inhibited in the regions of
290 Shh overexpression. Pax3 and Pax7 participate in the sonic hedgehog (Shh) signaling
291 pathway and are inhibited by Shh overexpression (Lin et al., 2016). Our previous
292 study indicated that the transcription factors Pax3 and Pax7 play important roles in
293 regulating morphogenesis and cell differentiation in the developing spinal cord (Lin et
294 al., 2016). Shh has also been shown to act as an axonal guidance molecule. Studies
295 have demonstrated that Shh attracts commissural axons at the ventral midline of the
296 developing spinal cord (Charron et al., 2003). In this study, we also showed that the
297 overexpression of Shh significantly inhibited the commissural axons from projecting
298 to the contralateral side. Our previous study indicated that the transcription factors
299 Pax3 play important roles in induces cell aggregation and perturbs commissural axon

bioRxiv preprint doi: https://doi.org/10.1101/178491; this version posted August 19, 2017. The copyright holder for this preprint (which was not certified by peer review) is the author/funder. All rights reserved. No reuse allowed without permission.

300 projection during embryonic spinal cord development (Lin et al., 2017). In this study
301 showed that the shh overexpression inhibited the expression of Pax3 and Pax7.
302 Therefore, the effect of Shh on the commissural axon projection may be related to the
303 effects of Shh on the expression of Pax3 and Pax7.
304 The current study provided evidence that Shh affects motor neuron positioning in the
305 spinal cord during chicken embryo development. The overexpression of Shh in the
306 spinal cord not only altered the positioning of the motor neurons, but also resulted in
307 the abnormal structure of the motor column. At the same time, Shh misexpression
308 inhibited the expression of genes related to the dorsal development and further
309 perturbed commissural axon projections during chicken embryo development.
310

311 **MATERIALS AND METHODS**

312 **Embryo and tissue preparation**

313 Fertilized eggs of Sea blue brownhad, obtained from a local farm (HWS-150,
314 JingHong, China) were incubated at 37.8 °C and 65% humidity. The Hamburger and
315 Hamilton (Hamburger V and Hamilton HL, 1992) system was used to stage the
316 embryos. The embryos were studied at stage 18 (E2.5) to stage 29 (E6), with at least
317 three embryos at each stage.

318 **In ovo electroporation**

319 The Shh overexpression plasmid was a gift by Redies (Prof. Christoph Redies ,
320 Institute of Anatomy I, Jena University Hospital, Teichgraben 7, D-07743 Jena,
321 Germany). The plasmid pCAGGS-GFP (green fluorescent protein) was derived by our
322 laboratory. All plasmids used were extracted with a kit (Cwbio, Beijing. China) and

bioRxiv preprint doi: https://doi.org/10.1101/178491; this version posted August 19, 2017. The copyright holder for this preprint (which was not certified by peer review) is the author/funder. All rights reserved. No reuse allowed without permission.

323 diluted in water.

324 The in ovo electroporation protocol was modified from our previous publications
325 (Luo et al., 2006; Yang et al., 2015; Lin et al., 2016). A stereomicroscope was used in
326 all the steps of the procedure. In brief, fertilized eggs were incubated until stage 18
327 (E2.5). Then, 3-4 mL of albumin was removed from the egg without disrupting the
328 yolk. Further, an incision into the shell was performed carefully using a pair of curved
329 scissors to obtain a 1-2-cm diameter window without touching the embryo. A mixture
330 of 4 μg/μL of pCAGGS-Shh, 0.25 μg/μL of pCAGGS-GFP plasmid, and Fast Green
331 dye (0.01%) or that of 0.25 μg/μL of pCAGGS-GFP plasmid as a control and Fast
332 Green dye (0.01%), were injected and loaded into the neural tube lumen using a
333 mouth pipette until the dye filled the entire space. The electrodes were then
334 immediately placed on both sides of the embryonic neural tube in parallel. A total of
335 six 18-volt pulses, which lasted for 60 ms, with a pause of 100 ms between each pulse,
336 were delivered. Bubbles near the electrodes indicated that the technique was
337 successfully performed. After the electroporation (CUY-21, Nepa Gene, Japan), the
338 electrodes were carefully removed, and the egg was sealed with a tape. The treated
339 eggs were then placed back in the incubator until they reached the desired stage for
340 sample collection, fixation, and analysis. For bromodeoxyuridine (BrdU) labeling, 5
341 μg/μL of BrdU was added into the embryo 24 hours prior to fixation.

342 **Tissue section**

343 When the embryos were at E6 (stage 26), samples of the spinal cord tissue were
344 collected. The embryos were fixed in 4% formaldehyde solution for 6-24 h,

bioRxiv preprint doi: https://doi.org/10.1101/178491; this version posted August 19, 2017. The copyright holder for this preprint (which was not certified by peer review) is the author/funder. All rights reserved. No reuse allowed without permission.

345 depending on their size. After fixation, the tissue was immersed in 18% sucrose
346 solution, embedded in Tissue-Tec O.C.T. compound (Sakura Finetek, USA), frozen in
347 liquid nitrogen, and stored at -80 °C until required. Samples were sectioned using a
348 cryotome (Leica 1850, Germany) and 20-μm thick sections were mounted on
349 Poly-L-lysine coated slides.

350 **cRNA probe synthesis and in situ hybridization**

351 Digoxigenin-labeled sense and antisense cRNA probes were transcribed in vitro using
352 purified PBS-SK plasmids containing the full-length Shh according to the
353 manufacturer's instructions (Roche, Germany). Sense cRNA probes were used as
354 negative controls for in situ hybridization.

355 For in situ hybridization, 20-μm thick cryosections were fixed with 4% formaldehyde
356 in PBS and pretreated with proteinase K and acetic anhydride. The sections were
357 hybridized overnight with a cRNA probe at a concentration of about 3 ng/μL at 70°C
358 in hybridization solution (50% formamide, 3× SSC, 10 mM EDTA, 10% dextran
359 sulfate, 1× Denhardt's solution, 42 μg/mL yeast transfer RNA and 42 μg/mL salmon
360 sperm DNA; Roche, Germany). The sections were washed to remove unbound cRNA
361 by RNase reaction, and then incubated with alkaline phosphatase-coupled
362 anti-digoxigenin Fab fragments (Roche, Germany) at 4°C overnight. For the
363 visualization of labeled mRNA, a substrate solution of nitroblue tetrazolium salt (NBT,
364 Fermentas, Lithuania) and 5-bromo-4-chloro-3-indoyl phosphate (BCIP, Fermentas,
365 Lithuania) were added.

366

bioRxiv preprint doi: https://doi.org/10.1101/178491; this version posted August 19, 2017. The copyright holder for this preprint (which was not certified by peer review) is the author/funder. All rights reserved. No reuse allowed without permission.

367 **Immunohistochemistry**

368 For immunohistochemistry, sections were fixed with 4% paraformaldehyde in PBS
369 for 15 min at 37°C. Following another TBS wash, a blocking solution (2% sheep
370 serum, 4% bovine serum albumin, 0.3% Triton X-100, and 0.1% sodium azide in
371 Tris-buffered saline, TBS, sheep serum and bovine serum albumin; Beijing Dingguo
372 co. LTD, China) was applied to tissue sections, for 1 h at room temperature. The
373 primary antibodies were then applied overnight at 4°C. The primary antibodies used
374 in the present study were rabbit anti Map2 polyclonal antibody (Abcam, United
375 Kingdom, 1:500 dilution), mouse anti chicken MNR2 monoclonal antibody (DSHB,
376 USA; 1:100 dilution), mouse anti Pax3 monoclonal antibody (DSHB, USA; 1:100
377 dilution), mouse anti Pax7 monoclonal antibody (DSHB, USA; 1:100 dilution), and
378 mouse anti BrdU monoclonal antibody (ZSGB-BIO, China; 1:100 dilution). For BrdU
379 detection, sections were incubated in 2 N HCl for 30 minutes followed by 0.1 M
380 $Na_2B_4O_7$ (pH 8.5), and then rinsed several times in TBS before the incubation with
381 anti-BrdU. Next, the appropriate goat-anti-rabbit Cy3-labeled (Jackson Immuno
382 Research, Europe Ltd, 1:1000 dilution), goat-anti-mouse Cy3-labeled (Jackson
383 Immuno Research, Europe Ltd, 1:1000 dilution) or goat-anti-rabbit FITC-labeled
384 (ZSGB-BIO, China; 1:100 dilution) secondary antibodies were applied for 2 h at 25°C.
385 A similar process was employed for double staining. Finally, DAPI
386 (4',6-diamidino-2-phenylindole, DAPI, Roche, Germany) was used to stain all cell
387 nuclei.

388 **Antibody characterization**

bioRxiv preprint doi: https://doi.org/10.1101/178491; this version posted August 19, 2017. The copyright holder for this preprint (which was not certified by peer review) is the author/funder. All rights reserved. No reuse allowed without permission.

389 See Table 1 for a list of all antibodies used. This study were used antibodies has been
390 described extensively. The staining patterns produced by all of the antibodies were
391 similar to those described previously.
392 Mouse monoclonal antibody against Pax3 was obtained from the Developmental
393 Studies Hybridoma Bank (catalogue no. pax3, RRID:AB_528426, mouse, monoclonal
394 antibody, IgG2a). To generate this antibody, the cDNA region that corresponded to
395 amino acids 298-481 of the C.terminal region of quail Pax3 was cloned by PCR into
396 the E. coli expression vector (Joven et al., 2013). Venters et al. (2004) confirmed that
397 the Pax3 antibody stains an single band of about 60 kDa on Western blots of extract
398 from E3 chicken neural tube and notochord. In addition, the expression pattern of
399 Pax3 protein obtained in the present study was similar to that reported previously for
400 Pax3 protein (Lin et al., 2017).
401 The mouse monoclonal antibody against Pax7 (DHSB, Catalogue No. pax7, RRID:
402 AB_528428) was generated by Dr. Atsushi Kawakami (Kawakami et al., 1997). The
403 DNA region corresponding to amino acids 352-523 of chick Pax7 was cloned by PCR
404 into the E. coli expression vector (Joven et al., 2013). Anti Pax7 antibody detects three
405 bands on Western blots of chicken brain tissue (Ferran et al., 2009). The staining
406 pattern of the Pax7 antibody obtained in the present study was the same as that
407 reported previously (Kobayashi et al., 2013; Lin et al., 2016).
408 The specificity of anti-MNR2 (81.5C10) was determine by comparison of the labeling
409 patterns obtained by immunohistochemistry and by in situ hybridization in the chick
410 embryo spinal cord (Tanabe et al., 1998). The staining pattern of the antibody in the

bioRxiv preprint doi: https://doi.org/10.1101/178491; this version posted August 19, 2017. The copyright holder for this preprint (which was not certified by peer review) is the author/funder. All rights reserved. No reuse allowed without permission.

411 this study was consistent with previous reports (Tanabe et al.,1998; Kobayashi et al.,
412 2013).
413 Anti-MAP2 was raised against rat microtubule-associated protein 2. Synthetic peptide
414 conjugated to KLH derived from within residues 1-100 of Rat MAP2. Anti MAP2
415 antibody detects two bands on Western blots of mouse brain tissue lysate total protein
416 (260,280 kDa). Additional bands at: 110 kDa,199 kDa,65 kDa are unsure as to the
417 identity of these extra bands (Sigma Product Sheet).
418 Monoclonal mouse anti-BrdU IgG1 (1:100; ZSGB-BIO, China, (ZM-0013), mouse,
419 monoclonal antibody, IgG1), recognizes BrdU. This antibody reacts with BrdU
420 incorporated into single-stranded DNA, attached to a protein carrier and free BrdU.
421 Table 1. Antibodies Used in This Study
422

Antigen	Immunogen	Detail of antibodies	Working dilution
Pax3	Chicken PAX3 (aa 298-481), recombinant protein made in E. coli	DSHB, USA, (PAX3), mouse, monoclonal antibody, IgG2a	1:100
Pax7	Chicken PAX7 (aa 352-523), recombinant protein made in E. coli	DSHB, USA, (PAX7), mouse, monoclonal antibody, IgG1	1:100
MNR2	C-terminal portion of chicken MNR2-GST fusion protein made in E. coli	DSHB, USA, (81.5C10) mouse, monoclonal antibody, IgG1	1:100
Map2	Rat microtubule associated protein 2	Abcam, United Kingdom, (ab32454), Rabbit, polyclonal	1:500
BrdU	BrdU（Bromodeoxyuridine）	ZSGB-BIO, China, (ZM-0013), mouse, monoclonal antibody, IgG1	1:100

423
424 **Microscopy**
425 The whole embryo was imaged under a stereo fluorescence microscope (LEICA

bioRxiv preprint doi: https://doi.org/10.1101/178491; this version posted August 19, 2017. The copyright holder for this preprint (which was not certified by peer review) is the author/funder. All rights reserved. No reuse allowed without permission.

426 M205FA, Germany) equipped with a digital camera (LEICA DFC425C, Germany). In
427 situ hybridization sections were viewed under a microscope (Nikon ECLIPSE 80i,
428 Japan), which was equipped with a digital camera (LEICA DFC300FX, Germany).
429 Immunohistochemistry sections were imaged under a confocal microscope (Olympus
430 ix81, Japan).

431 **Statistical analysis**

432 The average optical density and area of fluorescence intensity were calculated using
433 Plus Image-Pro 6 software (Media Cybernetics, USA), and the data were analyzed by
434 Statistics 17.0 SPSS software (IBM, USA). All data are presented as the mean ±
435 standard deviation (S.D.), of at least three independent experiments. The significance
436 of differences among the transfection groups was determined using ANOVA, where
437 p-value <0.05 was considered as significant.

438

439 **Competing interests**

440 The authors declare no competing financial interests.

441 **Author contributions**

442 Conceived and designed the experiments: Juntang Lin. Performed the experiments:
443 Ciqing Yang, Xiaoying Li, Qiuling Li, Qiong Li, Bichao Zhang. Analyzed the data: Han
444 Li, Ciqing Yang. Wrote the paper: Ciqing Yang.

445 **Funding**

446 This work was supported by the Henan Province University youth researcher support
447 program project (2015GGJS-133), the Henan Province Natural Science Foundation

bioRxiv preprint doi: https://doi.org/10.1101/178491; this version posted August 19, 2017. The copyright holder for this preprint (which was not certified by peer review) is the author/funder. All rights reserved. No reuse allowed without permission.

448 (162300410214; 162300410232; 162300410134), the support project for the
449 Disciplinary group of Psychology and Neuroscience, Xinxiang Medical University
450 (2016PN-KFKT-03), the Science and Technology Innovation Talents Support
451 Program of Henan Universities and Xinxiang City (14HASTIT032, CXRC16003), the
452 PhD Research Startup Foundation (505090) of Xinxiang Medical University, Henan
453 Key Laboratory of Medical Tissue Regeneration Open Project (KFKT15002) and
454 USM fellowship.

455 **References**

456 **Bonanomi, D. and Pfaff, S. L.** (2010). Motor axon pathfinding. Cold Spring Harb Perspect Biol
457 **2**:a001735.
458 **Bréjot, T., Blanchard, S., Hocquemiller, M., Haase, G., Liu, S., Nosjean, A., Heard, J. M. and**
459 **Bohl, D.** (2006). Forced expression of the motor neuron determinant HB9 in neural stem cells
460 affects neurogenesis. Exp Neurol **198,** 167-82.
461 **Briscoe, J. and Ericson, J.** (2001). Specification of neuronal fates in the ventral neural tube. Curr.
462 Opin. Neurobiol **11,** 43-49.
463 **Caceres, A., Mautino, J. and Kosik, K. S.** (1992). Suppression of MAP2 in cultured cerebellar
464 macroneurons inhibits minor neurite formation. Neuron **9,** 607-618.
465 **Cayuso, J., Ulloa, F., Cox, B., Briscoe, J. and Martí, E.** (2006). The Sonic hedgehog pathway
466 independently controls the patterning, proliferation and survival of neuroepithelial cells by
467 regulating Gli activity. Development **133,** 517-528.
468 **Chamberlain, C. E., Jeong, J., Guo, C., Allen, B. L. and McMahon, A. P.** (2008).
469 Notochord-derived Shh concentrates in close association with the apically positioned basal
470 body in neural target cells and forms a dynamic gradient during neural patterning.
471 Development **135,** 1097-1106.
472 **Charron, F., Stein, E., Jeong, J., McMahon, A. P. and Tessier-Lavigne, M.** (2003). The
473 morphogen sonic hedgehog is an axonal chemoattractant that collaborates with netrin-1 in
474 midline axon guidance. Cell **113,** 11-23.
475 **Chiang, C., Litingtung, Y., Lee, E., Young, K. E., Corden, J. L., Westphal, H. and Beachy, P.**
476 **A.** (1996). Cyclopia and defective axial patterning in mice lacking Sonic hedgehog gene
477 function. Nature **383,** 407-413.
478 **Echelard, Y., Epstein, D. J., St-Jacques, B., Shen, L., Mohler, J., McMahon, J. A. and**
479 **McMahon, A. P.** (1993). Sonic hedgehog, a member of a family of putative
480 signalingmolecules, is implicated in the regulation of CNS polarity. Cell **75,**1417-1430.
481 **Ericson, J., Morton, S., Kawakami, A., Roelink, H. and Jessell, T. M.** (1996). Two critical
482 periods of Sonic Hedgehog signaling required for the specification of motor neuron identity.
483 Cel **87,** 661-673.
484 **Ferran, J. L., de Oliveira, E. D., Merchan, P., Sandoval, J. E., Sanchez-Arrones, L.,**

bioRxiv preprint doi: https://doi.org/10.1101/178491; this version posted August 19, 2017. The copyright holder for this preprint (which was not certified by peer review) is the author/funder. All rights reserved. No reuse allowed without permission.

485 **Martinez-De-La-Torre, M. and Puelles, L.** (2009). Genoarchitectonic profile of developing
486 nuclear groups in the chicken pretectum. J Comp Neurol **517,**405-451.
487 **Hutchinson, S. A. and Eisen, J. S.** (2006). Islet1 and Islet2 have equivalent abilities to promote
488 motoneuron formation and to specify motoneuron subtype identity. Development **133,**
489 2137-2147.
490 **Jessell, T. M.** (2000). Neuronal specification in the spinal cord: inductive signals and
491 transcriptional codes. Nat. Rev. Genet **1,** 20-29.
492 **Joven, A., Morona, R., González, A. and Moreno, N.** (2013). Spatiotemporal patterns of Pax3,
493 Pax6, and Pax7 expression in the developing brain of a urodele amphibian, *Pleurodeles waltl.*
494 J Comp Neurol **521,** 3913-3953.
495 **Kalcheva, N., Albala, J., O'Guin, K., Rubino, H., Garner, C. and Shafit-Zagardo, B.** (1995).
496 Genomic structure of human microtubule-associated protein 2 (MAP-2) and characterization
497 of additional MAP-2 isoforms. Proc Natl Acad Sci U S A **92,** 10894-10898.
498 **Kania, A., Johnson, R. L. and Jessell, T. M.** (2000). Coordinate roles for LIM homeobox genes
499 in directing the dorsoventral trajectory of motor axons in the vertebrate limb. Cell
500 **102,**161-173.
501 **Kobayashi, N., Homma, S., Okada, T., Masuda, T., Sato, N., Nishiyama, K., Sakuma, C.,**
502 **Shimada, T. and Yaginuma, H.** (2013). Elucidation of target muscle and detailed
503 development of dorsal motor neurons in chick embryo spinal cord. J Comp Neurol **521,**
504 2987-3002.
505 **Krauss, S., Concordet, J. P. and Ingham, P. W.** (1993). A functionally conserved homologue of
506 the Drosophila segment polarity gene hedgehog is expressed in tissues with polarizing activity
507 in zebrafish embryos. Cell **75,** 1431-1444.
508 **Lee, J. J, von Kessler, D. P, Parks, S. and Beachy, P. A.** (1992). Secretion and localized
509 transcription suggest a role in positional signaling for products of the segmentation gene
510 hedgehog. Cell **71,** 33-50.
511 **Lehner, B., Sandner, B., Marschallinger, J., Lehner, C., Furtner, T., Couillard-Despres, S.,**
512 **Rivera, F. J., Brockhoff, G., Bauer, H. C., Weidner, N., et al.** (2011). The dark side of BrdU
513 in neural stem cell biology: detrimental effects on cell cycle, differentiation and survival. Cell
514 Tissue Res **345,** 313-328.
515 **Lin, J., Fu, S., Yang, C. and Redies, C.** (2017). Pax3 overexpression induces cell aggregation
516 and perturbs commissural axon projection during embryonic spinal cord development. J Comp
517 Neurol **525,**1618-1632.
518 **Lin, J., Wang, C., Yang, C., Fu, S. and Redies, C.** (2016). Pax3 and Pax7 interact reciprocally
519 and regulate the expression of cadherin-7 through inducing neuron differentiation in the
520 developing chicken spinal cord. J Comp Neurol **524,** 940-962.
521 **Luo, J., Ju, M. J. and Redies, C.** (2006). Regionalized cadherin-7 expression by radial glia is
522 regulated by Shh and Pax7 during chicken spinal cord development. Neuroscience
523 **142,**1133-1143.
524 **Luxey, M., Laussu, J. and Davy, A.** (2015). EphrinB2 sharpens lateral motor column division in
525 the developing spinal cord. Neural Dev **10,**25. doi: 10.1186/s13064-015-0051-9.
526 **Martí, E., Bumcrot, D. A., Takada, R. and McMahon, A. P.** (1995). Requirement of 19K form
527 of Sonic hedgehog for induction of distinct ventral cell types in CNS explants. Nature
528 **375,**322-325.

bioRxiv preprint doi: https://doi.org/10.1101/178491; this version posted August 19, 2017. The copyright holder for this preprint (which was not certified by peer review) is the author/funder. All rights reserved. No reuse allowed without permission.

529 **NUsslein-Volhard, C. and Wieschaus, E.** (1980). Mutations affecting segment number and
530 polarity in Drosophila. Nature **287,**795-801.
531 **Odden, J. P., Holbrook, S. and Doe, C. Q.** (2002). Drosophila HB9 is expressed in a subset of
532 motoneurons and interneurons, where it regulates gene expression and axon pathfinding. J
533 Neurosci **22,** 9143-9149.
534 **Otaegi, G., Pollock, A., Hong, J. and Sun, T.** (2011). MicroRNA miR-9 modifies motor neuron
535 columns by a tuning regulation of FoxP1 levels in developing spinal cords. J Neurosci
536 31,809-818.
537 **Patten, I. and Placzek, M.** (2000). The role of Sonic hedgehog in neural tube patterning. Cell
538 Mol Life Sci **57,**1695-1708.
539 **Peterson, K. A., Nishi, Y., Ma, W., Vedenko, A., Shokri, L., Zhang, X., McFarlane, M.,**
540 **Baizabal, J. M., Junker, J. P,, van Oudenaarden, A. et al.** (2012). Neural-specific Sox2
541 input and differential Gli-binding affinity provide context and positional information in
542 Shh-directed neural patterning. Genes Dev **26,**2802-2816.
543 **Placzek, M., Tessier-Lavigne, M., Yamada, T., Jessell, T. and Dodd, J.** (1990). Mesodermal
544 control of neural cell identity: floor plate induction by the notochord. Science **250,**985-988.
545 **Pringle, N. P., Yu, W. P., Guthrie, S., Roelink, H., Lumsden, A., Peterson, A. C. and**
546 **Richardson, W. D.** (1996). Determination of neuroepithelial cell fate: induction of the
547 oligodendrocyte lineage by ventral midline cells and sonic hedgehog. Dev Biol **177,**30-42.
548 **Ribes, V. and Briscoe, J.** (2009). Establishing and interpreting graded Sonic Hedgehog signaling
549 during vertebrate neural tube patterning: the role of negative feedback. Cold Spring Harb
550 Perspect Biol **1,**a002014. doi: 10.1101/cshperspect.a002014.
551 **Riddle, R., Johnson, R. L., Laufer, E. and Tabin, C.** (1993). Sonic hedgehog mediates the
552 polarizing activity of the ZPA. Cell **75,**1401-1416.
553 **Roelink, H., Augsberger, A., Heemskerk, J., Korzh, V., Norlin, S. and Ruiz iAltaba, A.** (1994).
554 Floor plate and motor neuron induction by Shh, avertebrate homolog of hedgehog expressed
555 by the notochord. Cell **76,**761-775.
556 **Rousso, D. L., Gaber, Z. B., Wellik, D., Morrisey, E. E. and Novitch, B. G.** (2008).
557 Coordinated actions of the forkhead protein Foxp1 and Hox proteins in the columnar
558 organization of spinal motor neurons. Neuron **59,**226-240.
559 **Santiago, C., Labrador, J. P. and Bashaw, G. J.** (2014). The homeodomain transcription factor
560 Hb9 controls axon guidance in Drosophila through the regulation of Robo receptors. Cell Rep
561 **7,**153-165.
562 **Tanabe, Y., Roelink, H. and Jessell, T. M.** (1995). Induction of motor neurons by sonic
563 hedgehog is independent of floor plate differentiation. Curr Biol **5,** 651–658.
564 **Tanabe, Y., William, C. and Jessell, T. M.** (1998). Specification of motor neuron identity by the
565 MNR2 homeodomain protein. Cell **95,**67-80.
566 **Tucker, R. P.** (1990). The roles of microtubule-associated proteins in brain morphogenesis: a
567 review. Brain Res Brain Res Rev **15,**101-120.
568 **Venters, S. J., Argent, R. E, Deegan, F. M, Perez-Baron, G., Wong, T. S., Tidyman, W. E.,**
569 **Denetclaw, W. F Jr, Marcelle, C., Bronner-Fraser, M. and Ordahl, CP.** (2004). Precocious
570 terminal differentiation of premigratory limb muscle precursor cells requires positive
571 signalling. Dev Dyn **229,**591-599.
572 **Vermot, J., Schuhbaur, B., Le, Mouellic, H., McCaffery, P., Garnier, J. M., Hentsch, D.,**

bioRxiv preprint doi: https://doi.org/10.1101/178491; this version posted August 19, 2017. The copyright holder for this preprint (which was not certified by peer review) is the author/funder. All rights reserved. No reuse allowed without permission.

573 **Brûlet, P., Niederreither, K., Chambon P, Dollé, P. and Le, Roux, I.** (2005). Retinaldehyde
574 dehydrogenase 2 and Hoxc8 are required in the murine brachial spinal cord for the
575 specification of Lim1+ motoneurons and the correct distribution of Islet1+ motoneurons.
576 Development **132,**1611-1621.
577 **Wilson, L. and Maden, M.** (2005). The mechanisms of dorsoventral patterning in the vertebrate
578 neural tube. Dev Biol **282,**1-13.
579 **Yamada, T., Pfaff, S. L., Edlund, T. and Jessell, T. M.** (1993).Control of cell pattern in the
580 neural tube: Motor neuron induction by diffusible factors from notochord and floor plate. Cell
581 **73,**673-686.
582 **Yamada, T., Placzek, M., Tanaka, H., Dodd, J. and Jessell, T. M.** (1991). Control of cell pattern
583 in the developing nervous system: Polarizing activity of the floor plate and notochord. Cell **64,**
584 635-647.
585 **Yang, C., Li, X., Liu, Y., Li, H., Guo, Z. and Lin, J.** (2015). Sonic hedgehog overexpression
586 regulates the neuroepithelial cells proliferation in the spinal cord of dorsal regions during
587 chicken embryo development. Neuro Endocrinol Lett **36,** 380-386.
588

589 **Figure legends:**

590 **Fig. 1 In situ hybridization demonstrates the overexpression of Shh**

591 A-C: Shh overexpression following pCAGGS-Shh and pCAGGS-GFP co-transfection; D-F:
592 Control group after pCAGGS-GFP transfection; A: at stage 24 (E4), B: at stage 27 (E5), C: at
593 stage 28 (E6), D: at stage 24 (E4), E: at stage 27 (E5), and F: at stage 28 (E6), Arrows (→)
594 indicate the areas of Shh overexpression. fp, floor plate; nc, notochord; sp, spinal cord; Scale bar =
595 100 μm in F for A-F.

596

597 **Fig. 2 The effect of Shh overexpression on microtubule-associated protein-2**
598 **(Map2) expression within the motor column in the developing chicken spinal**
599 **cord**

600 A-L: Shh overexpression following pCAGGS-Shh and pCAGGS-GFP co-transfection at 84 h.
601 DAPI nuclear staining (A, higher magnification of the ventral areas in E and I), GFP expression
602 (B, higher magnification of the ventral areas in F and J, green), Map2 expression (C, higher
603 magnification of the ventral areas in G and K, red), and merged images (D, higher magnification
604 of the ventral areas in H and L). M-X: Control group after pCAGGS-GFP transfection at 84 h.
605 DAPI nuclear stain (M, higher magnification of the ventral areas in Q and U), GFP expression (N,
606 higher magnification of the ventral areas in R and V), Map2 expression (O, higher magnification

bioRxiv preprint doi: https://doi.org/10.1101/178491; this version posted August 19, 2017. The copyright holder for this preprint (which was not certified by peer review) is the author/funder. All rights reserved. No reuse allowed without permission.

607 of the ventral areas in S and W, red), and the merged image (P, higher magnification of the ventral
608 areas in T and X). mc, motor column, sp, spinal cord. Arrows (→) indicate the areas of Map2
609 expression. Scale bars, 100 μm in A, E, I, M, Q, U for A-X, respectively.
610

611 **Fig. 3 The effect of Shh overexpression on motor neuron (MNR2) positioning**
612 **within the motor column in the chicken spinal cord**

613 A-H: Shh overexpression following pCAGGS-Shh and pCAGGS-GFP co-transfection at 84 h.
614 DAPI nuclear staining (A, higher magnification of the ventral areas in E), GFP expression (B,
615 higher magnification of the ventral areas in F, green), MNR2 expression (C, higher magnification
616 of the ventral areas in G, red), and merged images (D, higher magnification of the ventral areas in
617 H). I-P: Control group after pCAGGS-GFP transfection at 84 h. DAPI nuclear stain (I, higher
618 magnification of the ventral areas in M), GFP expression (J, higher magnification of the ventral
619 areas in N), MNR2 expression (K, higher magnification of the ventral areas in O, red), and the
620 merged image (L, higher magnification of the ventral areas in P). mc, motor column, Arrows (→)
621 indicate the areas of MNR2 expression. Scale bars, 100 μm in A, E, I, M for A-P, respectively.
622

623 **Fig. 4 The effect of Shh overexpression on neuroepithelial cell proliferation in the**
624 **spinal cord during chicken embryo development**

625 A-D: Shh overexpression following pCAGGS-Shh and pCAGGS-GFP co-transfection for 36 h.
626 DAPI nuclear staining (A), GFP expression (B, green), BrdU expression (C, red), and merged
627 images (D). E-H: Control group after pCAGGS-GFP transfection at 36 h. DAPI nuclear stain (E),
628 GFP expression (F), BrdU expression (red; G), and merged image (H). I-L: Shh overexpression
629 following pCAGGS-Shh and pCAGGS-GFP co-transfection at 84 h. DAPI nuclear staining (I,
630 higher magnification of the ventral areas in Q), GFP expression (J, higher magnification of the
631 ventral areas in R, green,), BrdU expression (K, higher magnification of the ventral areas in S,
632 red), and merged images (L, higher magnification of the ventral areas in T). M-P: Control group
633 after pCAGGS-GFP transfection at 84 h. DAPI nuclear stain (M, higher magnification of the
634 ventral areas in U), GFP expression (N, higher magnification of the ventral areas in V), BrdU
635 expression (O, higher magnification of the ventral areas in W, red), and merged image (P, higher

bioRxiv preprint doi: https://doi.org/10.1101/178491; this version posted August 19, 2017. The copyright holder for this preprint (which was not certified by peer review) is the author/funder. All rights reserved. No reuse allowed without permission.

636 magnification of the ventral areas in X). a, the pattern of spinal tissue slice section at 36 h. b, the
637 ratio of BrdU-positive cell numbers on the experimental side to those on the control side (E/C) at
638 24 h; c, the pattern of spinal tissue slice section at 84 h. d, the ratio of BrdU-positive cell numbers
639 on the experimental side to those on the control side (E/C) at 84 h; e, the pattern of spinal tissue
640 slice section in ventral areas at 84 h. f, the ratio of BrdU-positive cell numbers on the experimental
641 side to those on the control side (E/C) in ventral areas at 84 h. Data are presented as mean ± S.D.
642 **p<0.01. ne, neuroepithelial cells. Scale bars, 100 μm in A, E, I, M, Q, U for A-X, respectively.
643

644 **Fig. 5 The effect of Shh overexpression on Pax3 and Pax7 expression in the spinal**
645 **cord during chicken embryo development**

646 A-F: Shh overexpression group with pCAGGS-Shh and pCAGGS-GFP plasmid co-transfection,
647 showing GFP (A, higher magnification in D), Pax3 (B, higher magnification in E) expression, and
648 merged image (C, higher magnification in F). G-L: Control group with pCAGGS-GFP plasmid
649 transfection, showing GFP (G, higher magnification in J), Pax3 (H, higher magnification in K)
650 expression, and merged image (I, higher magnification in L). M-R: Shh overexpression group with
651 pCAGGS-Shh and pCAGGS-GFP plasmid co-transfection, showing GFP (M, higher
652 magnification in P), Pax7 (N, higher magnification in Q) expression, and merged image (O, higher
653 magnification in R). S-X: Control group with pCAGGS-GFP plasmid transfection, showing GFP
654 (S, higher magnification in V), Pax7 (T, higher magnification in W) expression, and merged image
655 (U, higher magnification in X). a, the pattern of spinal tissue slice section. b, the mean optical
656 density ratio of the experimental side to the control side; c, the mean optical density ratio of the
657 experimental side to the control side; d, percentage of GFP positive axonal area projecting to the
658 contralateral side (%). Data are presented as mean ± S.D. **p<0.01. drg, dorsal root ganglion; sp,
659 spinal cord. Arrows (→) indicate the areas of Pax3 or Pax7 expression. Scale bars, 100 μm in A, D,
660 G, J for A-L. 100 μm in M, P, S, V for M-X, respectively.

661 **Fig. 6 The effect of shh overexpression on commissural axons projection in the**
662 **spinal cord during chicken embryo development**

663 Rostro-caudal series of transverse sections after electroporation of the shh overexpression (shh
664 overexpression; A-G); H, the pattern of commissural axons projection. The GFP alone expression

bioRxiv preprint doi: https://doi.org/10.1101/178491; this version posted August 19, 2017. The copyright holder for this preprint (which was not certified by peer review) is the author/funder. All rights reserved. No reuse allowed without permission.

665 (control; I-O); P, the pattern of commissural axons projection. In ovo electroporation was
666 performed at E2.5 (2.5 days' incubation) and the positive embryos were collected at E6.
667 Abbreviations: fp, floor plate; ilc, intermediate longitudinal commissural axons; mlc, medial
668 longitudinal commissural axons; rp, roof plate. Scale bar: 100μm in O for A-G and I-O.
669

Shh over-expression

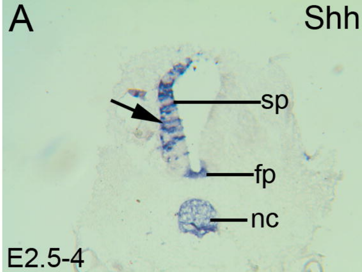

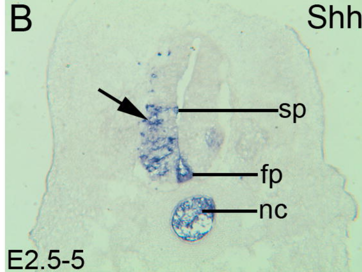

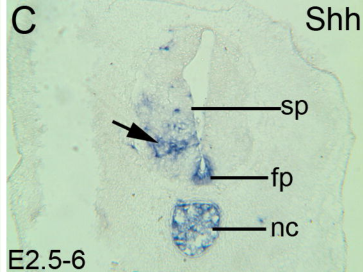

Control

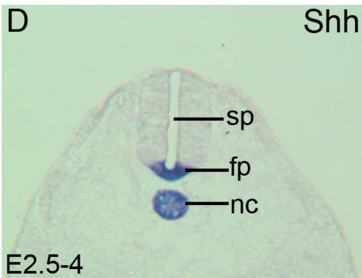

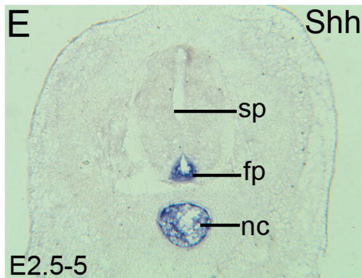

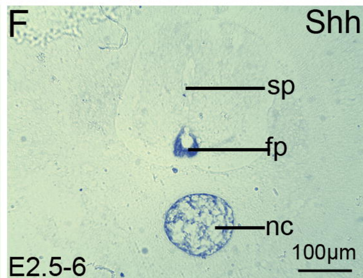

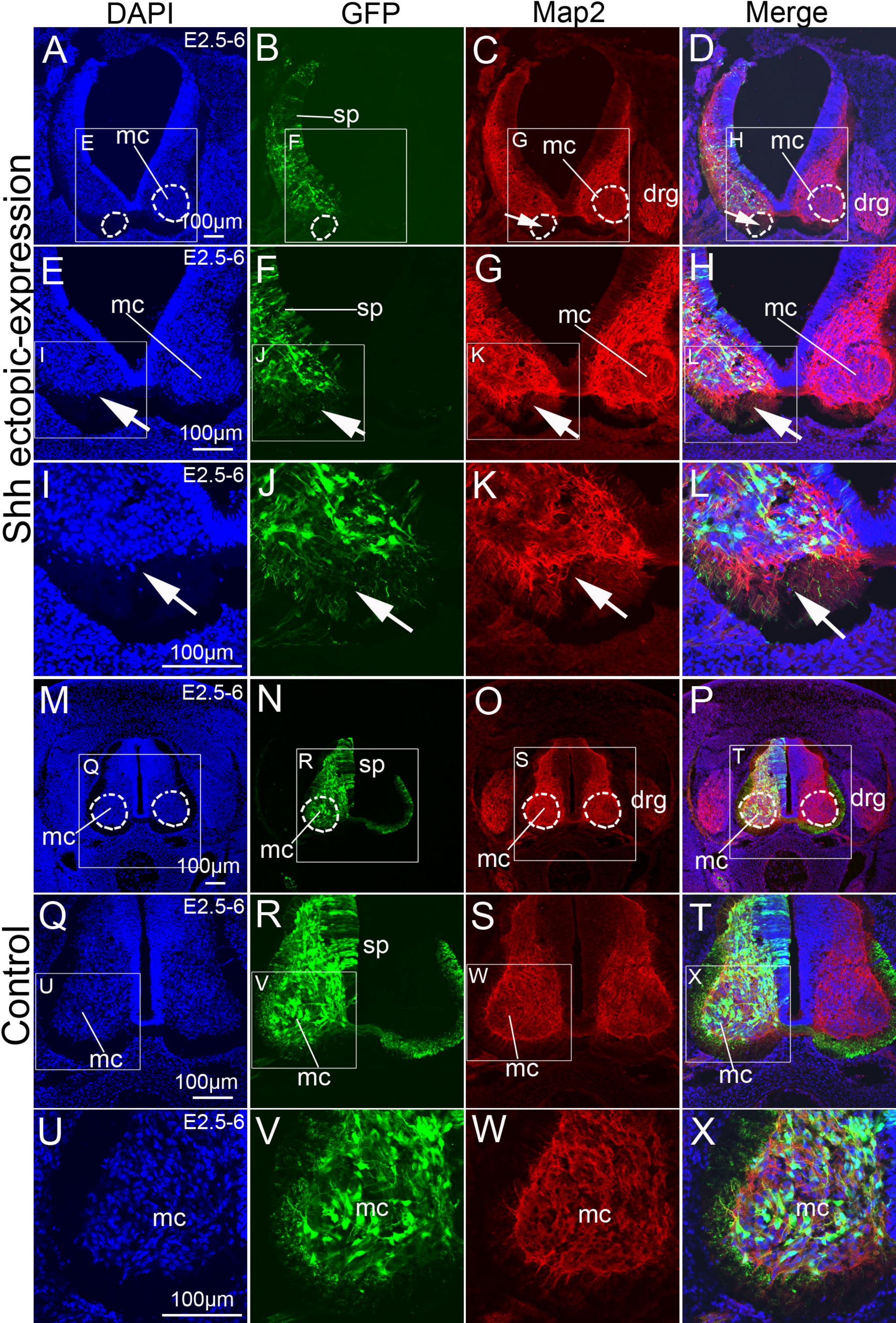

DAPI
GFP
Map2
Merge
Shh ectopic-expression
Control
A
E2.5-6
E
mc
100µm
B
sp
F
C
G
mc
drg
D
H
mc
drg
E
E2.5-6
mc
I
100µm
F
sp
J
G
mc
K
H
mc
L
I
E2.5-6
100µm
J
K
L
M
E2.5-6
Q
mc
100µm
N
R
sp
mc
O
S
drg
mc
P
T
drg
mc
Q
E2.5-6
U
mc
100µm
R
sp
V
mc
S
W
mc
T
X
mc
U
E2.5-6
mc
100µm
V
mc
W
mc
X
mc

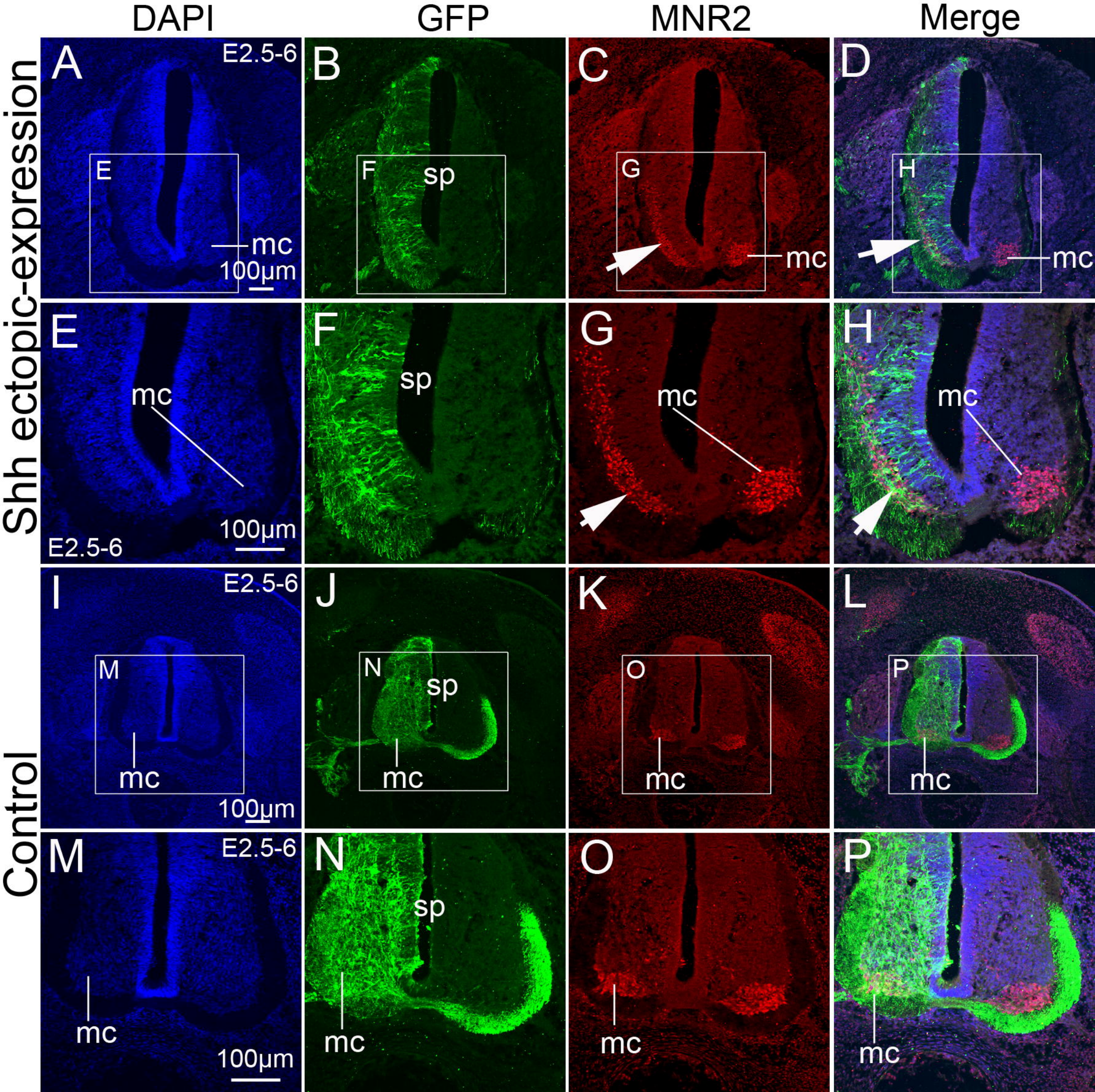
DAPI
GFP
MNR2
Merge
Shh ectopic-expression
Control
A
E2.5-6
E
mc
100μm
B
F
sp
C
G
mc
D
H
mc
E
mc
100μm
E2.5-6
F
sp
G
mc
H
mc
I
E2.5-6
M
mc
100μm
J
N
sp
mc
K
O
mc
L
P
mc
M
E2.5-6
mc
100μm
N
sp
mc
O
mc
P
mc

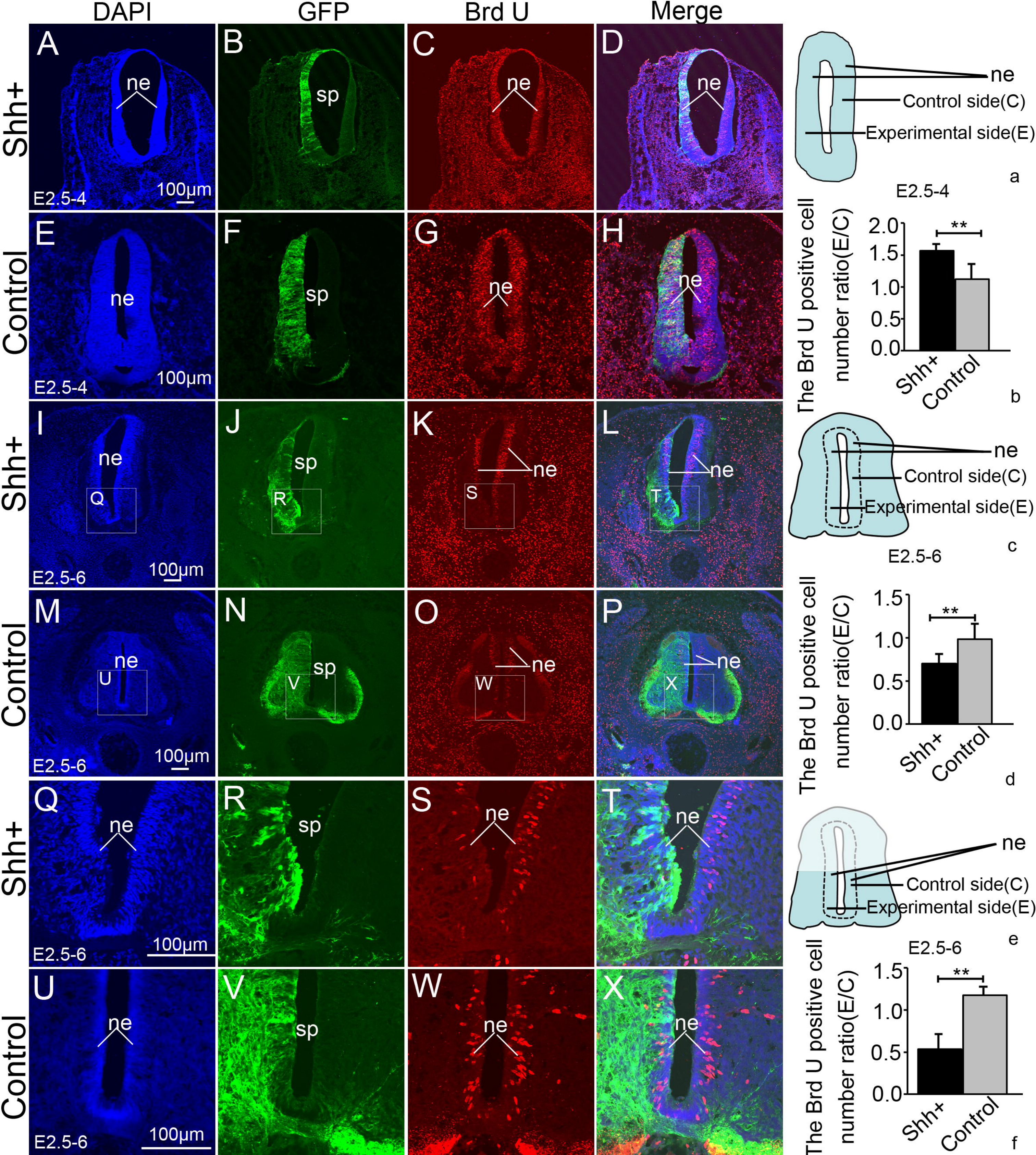
DAPI
GFP
Brd U
Merge
Shh+
Control
Shh+
Control
Shh+
Control
A
B
C
D
E
F
G
H
I
J
K
L
M
N
O
P
Q
R
S
T
U
V
W
X
ne
sp
E2.5-4
E2.5-6
100μm
Control side(C)
Experimental side(E)
a
b
c
d
e
f
The Brd U positive cell number ratio(E/C)
**
2.0
1.5
1.0
0.5
0.0
Shh+
Control

GFP Pax3 Merge GFP Pax7 Merge

Shh ectopic-expression

Control

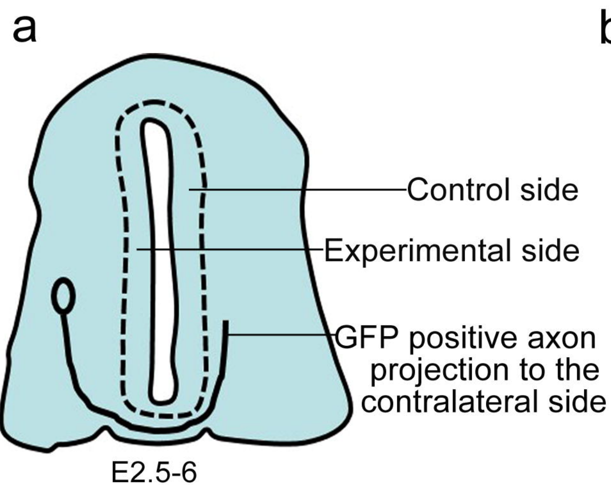

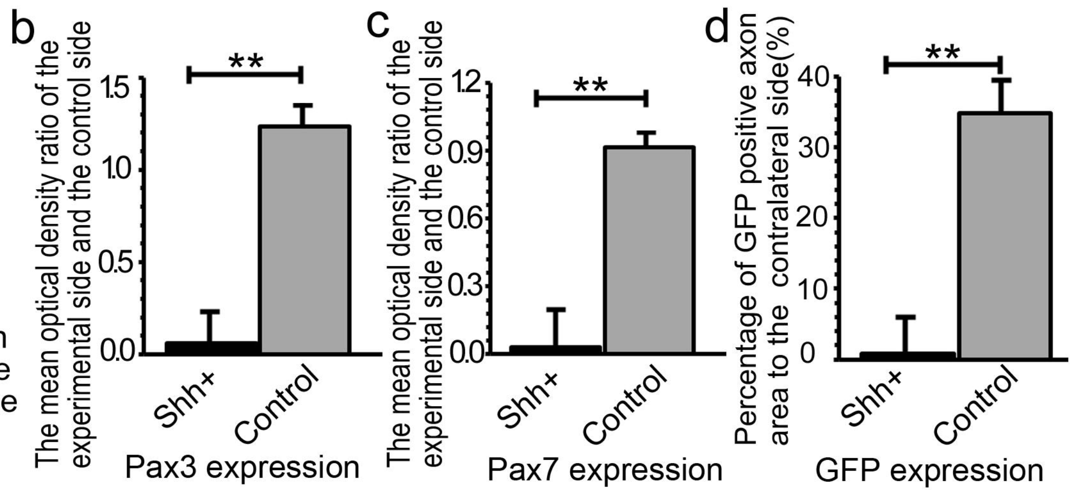

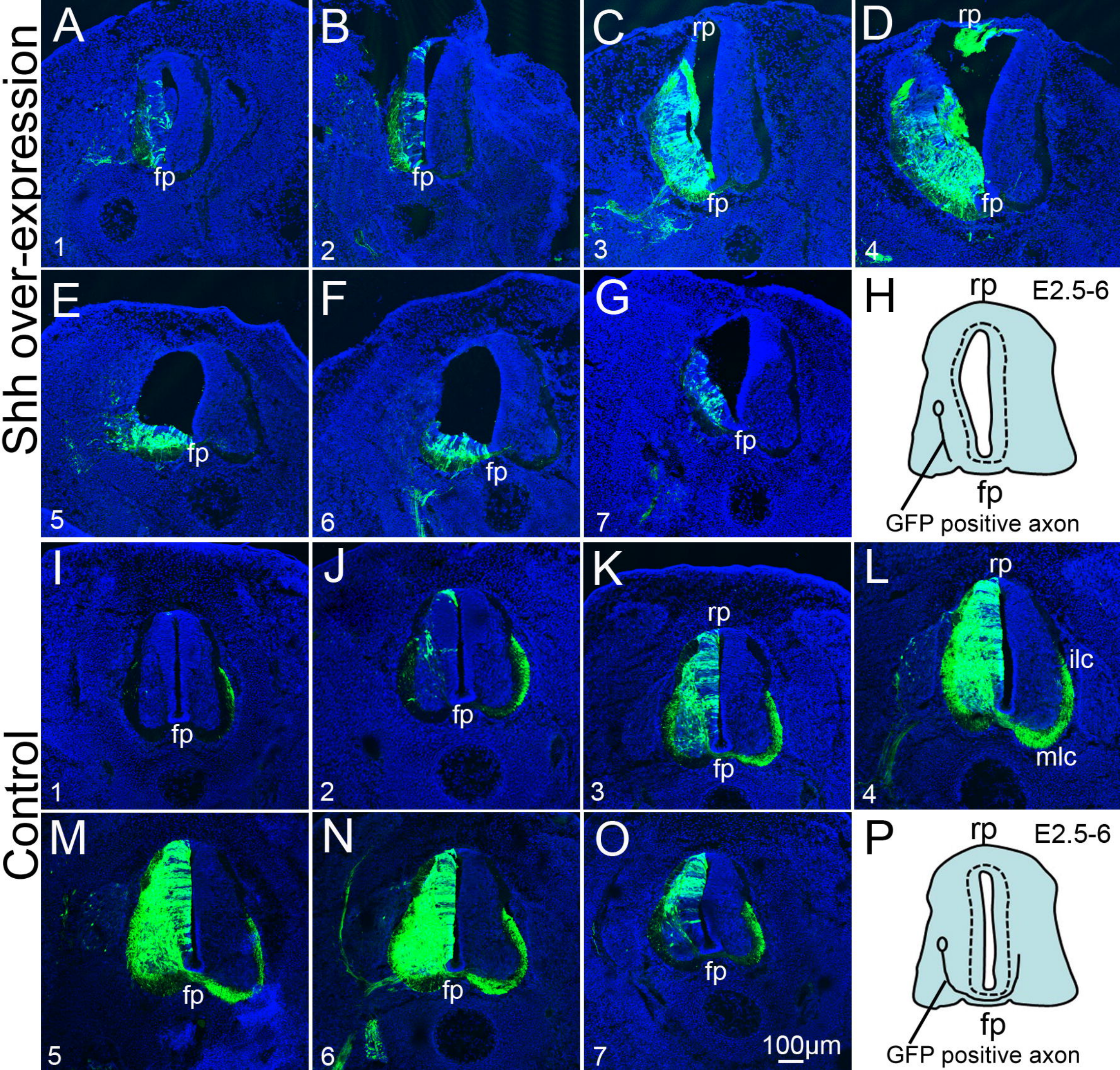

Shh over-expression
Control
A
B
C
D
E
F
G
H
I
J
K
L
M
N
O
P
fp
rp
1
2
3
4
5
6
7
E2.5-6
GFP positive axon
ilc
mlc
100μm